Mikko Lyly and Rolf Stenberg

STABILIZED MITC PLATE BENDING ELEMENTS

To appear in: *Proceedings of the Second International Conference on Computational Structures Technology, Athens Greece 30.8.-1.9.1994*

Abstract

We propose three new families of elements for the Reissner-Mindlin plate model. In the methods the MITC interpolation technique for the shear term is combined with a recent stabilization technique [11]. By this we obtain methods that are stable and in which the same basis functions can be used for the deflection and the rotation.

1 Introduction

As is well known, the Reissner-Mindlin plate bending equations cannot be used as such in the finite element method with low order elements. This is due to the locking of the deflection and an oscillating shear force. The usual remedy is to modify the shear energy by using various reduction techniques to mollify the limiting Kirchhoff constraint. It has, however, been possible to rigorously analyze very few of these methods. The only whole family of methods (i.e. methods for all polynomial degrees) that has been shown to converge optimally is the MITC family, cf. [2, 5]. In this family of methods the spaces for the deflection and rotation have to be chosen very carefully in order to satisfy the necessary stability conditions.

Our approach consists of combining the covariant interpolation operator used in MITC family with a stabilization technique introduced in [11]. By this we obtain several stable and optimally convergent families of methods.

Compared to the original MITC methods our approach has the following advantages. It is possible to obtain stable linear and bilinear elements. (These elements have earlier been presented in [5, 8].) In the methods identical finite element spaces are used for the deflection and both components of the rotation. Furhermore, the methods give stiffness matrices which are better conditioned than those of the original MITC elements. This can be an advantage when solving the problem iteratively (cf. [6] where this idea has been used in connection with multigrid methods).

In the next section we will recall the plate bending model. In Section 3 we will describe the finite element methods and give the results of the theoretical analysis. The final section is devoted to some numerical tests.

2 Notation and preliminaries

We will consider the Reissner-Mindlin plate bending model and assume that the plate is clamped along its boundary. Denoting the midsurface of the plate by $\Omega \subset \mathbb{R}^2$, the variational problem is: find the deflection $w \in H_0^1(\Omega)$ and the rotation vector $\boldsymbol{\beta} \in [H_0^1(\Omega)]^2$ such that

$$Gt^3 a(\boldsymbol{\beta},\boldsymbol{\eta}) + G\kappa t(\nabla w - \boldsymbol{\beta}, \nabla v - \boldsymbol{\eta}) = (f,v) \quad \forall (v,\boldsymbol{\eta}) \in [H_0^1(\Omega)]^3. \tag{1}$$

Here G is the shear modulus and κ denotes the shear correction factor. f is the transverse load and t is the thickness of the plate. The bilinear form a is defined as

$$a(\boldsymbol{\beta},\boldsymbol{\eta}) = \frac{1}{6}\big\{(\boldsymbol{\varepsilon}(\boldsymbol{\beta}),\boldsymbol{\varepsilon}(\boldsymbol{\eta})) + (\frac{\nu}{1-\nu})(\operatorname{div}\boldsymbol{\beta},\operatorname{div}\boldsymbol{\eta})\big\}, \tag{2}$$

where $\boldsymbol{\varepsilon}(\cdot)$ is the small strain tensor and ν is the Poisson ratio. As usual, the L_2-inner products are denoted by $(\cdot,\cdot)_D$ and the corresponding norms by $\|\cdot\|_{0,D}$, with the subscript D dropped when $D = \Omega$.

The shear force $\boldsymbol{Q}$ and bending moment $\boldsymbol{M}$ are obtained from

$$\boldsymbol{Q} = G\kappa t(\nabla w - \boldsymbol{\beta}) \tag{3}$$

and

$$\boldsymbol{M} = \frac{Gt^3}{6}\big\{\boldsymbol{\varepsilon}(\boldsymbol{\beta}) + (\frac{\nu}{1-\nu})\operatorname{div}\boldsymbol{\beta}\ \boldsymbol{I}\big\}, \tag{4}$$

respectively

For the theoretical analysis one assumes that the load is proportional to the third power of the plate thickness, i.e. $f = Gt^3 g$ with g fixed independent of t. With this assumption the problem (1) has a finite and non-trivial solution in limit when $t \to 0$ (cf. [4]). Hence, the problem becomes: find $(w,\boldsymbol{\beta}) \in [H_0^1(\Omega)]^3$ such that

$$a(\boldsymbol{\beta},\boldsymbol{\eta}) + \kappa t^{-2}(\nabla w - \boldsymbol{\beta}, \nabla v - \boldsymbol{\eta}) = (g,v) \quad \forall (v,\boldsymbol{\eta}) \in [H_0^1(\Omega)]^3. \tag{5}$$

Introducing the scaled shear force

$$\boldsymbol{q} = \kappa t^{-2}(\nabla w - \boldsymbol{\beta}) \tag{6}$$

as an independent unknown, the mixed form of (5) is: find $(w,\boldsymbol{\beta},\boldsymbol{q}) \in [H_0^1(\Omega)]^3 \times [L_2(\Omega)]^2$ such that

$$a(\boldsymbol{\beta},\boldsymbol{\eta}) + (\boldsymbol{q}, \nabla v - \boldsymbol{\eta}) = (g,v) \quad \forall (v,\boldsymbol{\eta}) \in [H_0^1(\Omega)]^3 \tag{7}$$

$$\kappa^{-1}t^2(\boldsymbol{q},\boldsymbol{s}) - (\nabla w - \boldsymbol{\beta}, \boldsymbol{s}) = 0 \quad \forall \boldsymbol{s} \in [L_2(\Omega)]^2. \tag{8}$$

The strong form corresponding to this system is obtained by integrating by parts:

$$\begin{aligned} \boldsymbol{L}\boldsymbol{\beta} + \boldsymbol{q} &= \boldsymbol{0} \quad \text{in } \Omega, \\ -\operatorname{div} \boldsymbol{q} &= g \quad \text{in } \Omega, \\ -\kappa^{-1} t^2 \boldsymbol{q} + \nabla w - \boldsymbol{\beta} &= \boldsymbol{0} \quad \text{in } \Omega, \\ w &= 0 \quad \text{on } \partial\Omega, \\ \boldsymbol{\beta} &= \boldsymbol{0} \quad \text{on } \partial\Omega. \end{aligned} \tag{9}$$

Above the differential operator $\boldsymbol{L}$ is defined through

$$\boldsymbol{L}\boldsymbol{\eta} = \frac{1}{6} \mathbf{div} \left\{ \varepsilon(\boldsymbol{\eta}) + (\frac{\nu}{1-\nu}) \operatorname{div} \boldsymbol{\eta}\ \boldsymbol{I} \right\}, \tag{10}$$

where **div** stands for the divergence of second order tensors and $\boldsymbol{I}$ is the unit tensor.

3 The finite element methods

We let $\mathcal{C}_h$ be the finite element partitioning of $\bar{\Omega}$ into triangles or convex quadrilaterals and define the finite element subspaces for the deflection and rotation vector with the index $k \geq 1$ as

$$W_h = \{ v \in H_0^1(\Omega) \mid v_{|K} \in R_k(K),\ \forall K \in \mathcal{C}_h \}, \tag{11}$$

$$\boldsymbol{V}_h = \{ \boldsymbol{\eta} \in [H_0^1(\Omega)]^2 \mid \boldsymbol{\eta}_{|K} \in [R_k(K)]^2,\ \forall K \in \mathcal{C}_h \}. \tag{12}$$

We point out that this means that equal basis functions are used for the deflection and both component of the rotation.

The shear energy will be modified by interpolating with the MITC technique. For an element $K \in \mathcal{C}_h$ an auxiliary space $\boldsymbol{\Gamma}_k(K)$ and an MITC reduction operator $\boldsymbol{R}_K : [H^1(K)]^2 \to \boldsymbol{\Gamma}_k(K)$ are introduced.

The finite element methods for the problem (1) are then defined as follows: find $(w_h, \boldsymbol{\beta}_h) \in W_h \times \boldsymbol{V}_h$ such that

$$\mathcal{B}_h(w_h, \boldsymbol{\beta}_h; v, \boldsymbol{\eta}) = (f, v) \quad \forall (v, \boldsymbol{\eta}) \in W_h \times \boldsymbol{V}_h. \tag{13}$$

The bilinear form $\mathcal{B}_h$ is defined as

$$\begin{aligned} \mathcal{B}_h(w, \boldsymbol{\beta}; v, \boldsymbol{\eta}) = Gt^3 \big\{ & a(\boldsymbol{\beta}, \boldsymbol{\eta}) - \alpha \sum_{K \in \mathcal{C}_h} h_K^2 (\boldsymbol{L}\boldsymbol{\beta}, \boldsymbol{L}\boldsymbol{\eta})_K \\ & + \sum_{K \in \mathcal{C}_h} \kappa (t^2 + \kappa\alpha h_K^2)^{-1} b_K(w, \boldsymbol{\beta}; v, \boldsymbol{\eta}) \big\}, \end{aligned} \tag{14}$$

with

$$\begin{aligned} & b_K(w, \boldsymbol{\beta}; v, \boldsymbol{\eta}) = \\ & (\nabla w - \boldsymbol{R}_K \boldsymbol{\beta} - \alpha h_K^2 \boldsymbol{L}\boldsymbol{\beta}, \nabla v - \boldsymbol{R}_K \boldsymbol{\eta} - \alpha h_K^2 \boldsymbol{L}\boldsymbol{\eta})_K. \end{aligned} \tag{15}$$

Here h_K denotes the diameter of the element $K \in \mathcal{C}_h$ and α is a positive constant for which an upper bound will be defined below.

The different methods will then be defined by specifying the spaces $R_k(K)$ and $\boldsymbol{\Gamma}_k(K)$ together with the reduction operator $\boldsymbol{R}_K$.

From the solution $(w_h, \boldsymbol{\beta}_h)$ to (13), the approximations for the shear force and bending moment are obtained from

$$\boldsymbol{Q}_{h|K} = \frac{G\kappa t^3}{t^2 + \kappa\alpha h_K^2} (\nabla w_h - \boldsymbol{R}_K \boldsymbol{\beta}_h - \alpha h_K^2 \boldsymbol{L}\boldsymbol{\beta}_h)_{|K}$$

and

$$\boldsymbol{M}_{h|K} = \frac{Gt^3}{6} \big\{ \varepsilon(\boldsymbol{\beta}_h) + (\frac{\nu}{1-\nu}) \operatorname{div} \boldsymbol{\beta}_h\ \boldsymbol{I} \big\}_{|K} \quad \forall K \in \mathcal{C}_h, \tag{16}$$

respectively. An alternative way to determine the approximate shear force is to calculate it through the equilibrium equation

$$\boldsymbol{Q}_{h|K} = -Gt^3 \boldsymbol{L}\boldsymbol{\beta}_{h|K}, \quad \forall K \in \mathcal{C}_h. \tag{17}$$

This is, of course, possible only when $k \geq 2$.

Since $\boldsymbol{Q}_h$ and $\boldsymbol{M}_h$ are discontinuous, it is customary to "smooth" them e.g. by projecting onto some suitably chosen finite element space consisting of continuous functions. This we do by letting

$$S_h = \{ s \in C(\bar{\Omega}) \mid s_{|K} \in R_k(K),\ \forall K \in \mathcal{C}_h \} \tag{18}$$

and then defining the smoothed shear force $\boldsymbol{Q}_h^* \in [S_h]^2$ and bending moment $\boldsymbol{M}_h^* \in [S_h]^{2\times 2}$ through

$$(\boldsymbol{Q}_h^*, \boldsymbol{s}) = (\boldsymbol{Q}_h, \boldsymbol{s}), \quad \forall \boldsymbol{s} \in [S_h]^2, \tag{19}$$

and

$$(\boldsymbol{M}_h^*, \boldsymbol{r}) = (\boldsymbol{M}_h, \boldsymbol{r}), \quad \forall \boldsymbol{r} \in [S_h]^{2\times 2}. \tag{20}$$

Next, let us turn to the different methods.

Method I

We let K be a triangle, $R_k(K) = P_k(K)$ with $k \geq 1$ and denote by

$$\boldsymbol{\Gamma}_k(K) = [P_{k-1}(K)]^2 \oplus (y, -x) \tilde{P}_{k-1}(K), \tag{21}$$

the rotated Raviart-Thomas space [10]. Here $\tilde{P}_{k-1}(K)$ is the space of homogeneous polynomials of degree $k-1$. The reduction operator is defined through the conditions

$$\begin{aligned} & \int_E [(\boldsymbol{R}_K \boldsymbol{\eta} - \boldsymbol{\eta}) \cdot \boldsymbol{\tau}] v\ ds = 0,\ \forall v \in P_{k-1}(E) \\ & \qquad \text{for every edge } E \text{ of } K, \end{aligned} \tag{22}$$

and for $k \geq 2$

$$\int_K (\boldsymbol{R}_K \boldsymbol{\eta} - \boldsymbol{\eta}) \cdot \boldsymbol{r}\ dxdy = 0,\ \forall \boldsymbol{r} \in [P_{k-2}(K)]^2. \tag{23}$$

Above $\boldsymbol{\tau}$ is the tangent to the edge E.

Remark 1. For linear elements with $k = 1$ it holds

$$\boldsymbol{L}\boldsymbol{\eta}_{|K} = \boldsymbol{0}, \quad \forall K \in \mathcal{C}_h, \quad \forall \boldsymbol{\eta} \in \boldsymbol{V}_h, \tag{24}$$

and so the bilinear form $\mathcal{B}_h$ reduces to

$$\begin{aligned} \mathcal{B}_h(w, \boldsymbol{\beta}; v, \boldsymbol{\eta}) = Gt^3 \big\{ & a(\boldsymbol{\beta}, \boldsymbol{\eta}) \\ & + \sum_{K \in \mathcal{C}_h} \frac{\kappa}{t^2 + \kappa\alpha h_K^2} (\nabla w - \boldsymbol{R}_K \boldsymbol{\beta}, \nabla v - \boldsymbol{R}_K \boldsymbol{\eta})_K \big\}. \end{aligned} \tag{25}$$

This gives the linear element introduced in [5]. Taking $\alpha = 0$ we get a linear element of Hughes and Taylor [7], which is not stable.

Remark 2. In our numerical computations we also give the results obtained with the MITC7 element [1] which is obtained from Method I by choosing $\alpha = 0$, $k = 2$ and

taking $R_2(K) = P_2(K) \oplus \text{span}\{\lambda_1\lambda_2\lambda_3\}$ in the rotation space $\boldsymbol{V}_h$. Here λ_i, $i = 1,2,3$, denote the barycentric coordinates of K.

Remark 3. With $\alpha = 0$ and $k = 2$ one obtains an (unstable) element proposed in [9].

Method II

Now K is a quadrilateral and $R_k(K) = Q_k(K)$ with $k \geq 1$. We let $\boldsymbol{J}_K$ be the Jacobian matrix of the mapping $\boldsymbol{F}_K : \hat{K} \rightarrow K$ ($\hat{K}$ is the unit square with coordinates ξ and η) and define

$$\boldsymbol{\Gamma}_k(K) = \{\boldsymbol{\eta} \mid \boldsymbol{\eta} = \boldsymbol{J}_K^{-T}\hat{\boldsymbol{\eta}} \circ \boldsymbol{F}_K^{-1},\ \hat{\boldsymbol{\eta}} \in \boldsymbol{\Gamma}_k(\hat{K})\}, \tag{26}$$

where $\boldsymbol{J}_K^{-T}$ is the transpose of $\boldsymbol{J}_K^{-1}$, and

$$\boldsymbol{\Gamma}_k(\hat{K}) = P_{k-1,k}(\hat{K}) \times P_{k,k-1}(\hat{K}). \tag{27}$$

This is the rectangular rotated Raviart-Thomas space with

$$P_{m,n}(\hat{K}) = \{v \mid v = \sum_{i=0}^{m}\sum_{j=0}^{n} a_{ij}\xi^i\eta^j \text{ for some } a_{ij} \in \mathbb{R}\}. \tag{28}$$

The reduction operator $\boldsymbol{R}_K : [H^1(K)]^2 \rightarrow \boldsymbol{\Gamma}_k(K)$ is now defined through

$$\boldsymbol{R}_K\boldsymbol{\eta} = \boldsymbol{J}_K^{-T}\boldsymbol{R}_{\hat{K}}\boldsymbol{J}_K^T\boldsymbol{\eta}, \tag{29}$$

where $\boldsymbol{R}_{\hat{K}} : [H^1(\hat{K})]^2 \rightarrow \boldsymbol{\Gamma}_k(\hat{K})$ is an operator satisfying the conditions

$$\int_{\hat{E}} [(\boldsymbol{R}_{\hat{K}}\hat{\boldsymbol{\eta}} - \hat{\boldsymbol{\eta}}) \cdot \boldsymbol{\tau}] v \ ds = 0,\ \forall v \in P_{k-1}(\hat{E}) \quad \text{for every edge } \hat{E} \text{ of } \hat{K}, \tag{30}$$

and in the case if $k \geq 2$

$$\int_{\hat{K}} (\boldsymbol{R}_{\hat{K}}\hat{\boldsymbol{\eta}} - \hat{\boldsymbol{\eta}}) \cdot \boldsymbol{r} \ d\xi d\eta = 0, \quad \forall \boldsymbol{r} \in P_{k-1,k-2}(\hat{K}) \times P_{k-2,k-1}(\hat{K}). \tag{31}$$

Remark 4. If $k = 1$ it is possible use the reduced bilinear form (25). By doing this we get the stabilized MITC4 element [8], and if we take $\alpha = 0$, the original MITC4 element of Bathe and Dvorkin [3].

Method III

Again, K is a quadrilateral but now we choose $R_k(K) = Q_k^r(K) = Q_k(K) \cap P_{k+1}(K)$ (isoparametric) with $k \geq 1$. For this method we define

$$\boldsymbol{\Gamma}_k(\hat{K}) = [P_k(\hat{K})]^2 \setminus \text{span}\{(\xi^k, 0), (0, \eta^k)\}, \tag{32}$$

which is the rotated rectangular Brezzi-Douglas-Fortin-Marini (BDFM) space [6]. The operator $\boldsymbol{R}_K$ is defined as in (29) with $\boldsymbol{R}_{\hat{K}}$ satisfying

$$\int_{\hat{E}} [(\boldsymbol{R}_{\hat{K}}\hat{\boldsymbol{\eta}} - \hat{\boldsymbol{\eta}}) \cdot \boldsymbol{\tau}] v \ ds = 0,\ \forall v \in P_{k-1}(\hat{E}) \quad \text{for every edge } \hat{E} \text{ of } \hat{K}, \tag{33}$$

and for $k \geq 2$

$$\int_{\hat{K}} (\boldsymbol{R}_{\hat{K}}\hat{\boldsymbol{\eta}} - \hat{\boldsymbol{\eta}}) \cdot \boldsymbol{r} \ d\xi d\eta = 0,\ \forall \boldsymbol{r} \in [P_{k-2}(\hat{K})]^2. \tag{34}$$

Remark 5. The MITC9 element [1] is obtained from Method III by taking $\alpha = 0$, $k = 2$ and $R_2(K) = Q_2(K)$ in the rotation space $\boldsymbol{V}_h$.

For the methods it is possible to prove the stability and optimal error estimates. These are valid if the parameter α is in the range $0 < \alpha < C_I$, where C_I is the constant in the following inverse inequality

$$C_I \sum_{K \in \mathcal{C}_h} h_K^2 ||\boldsymbol{L}\boldsymbol{\eta}||_{0,K}^2 \leq a(\boldsymbol{\eta}, \boldsymbol{\eta}), \quad \forall \boldsymbol{\eta} \in \boldsymbol{V}_h. \tag{35}$$

Due to (24) there is no upper limit for α for the linear triangular element. The same applies for the stabilized bilinear MITC4 based on the bilinear form (25).

The error analysis is done for the scaled problem (5). For this we define the scaled moment tensor $\boldsymbol{m}$ by $\boldsymbol{M} = Gt^3\boldsymbol{m}$. With some assumptions on the regularity of the exact solution we can prove the following error estimates

$$\|w - w_h\|_0 \leq Ch^{k+1}, \tag{36}$$

$$\|\boldsymbol{m} - \boldsymbol{m}_h\|_0 \leq Ch^k, \tag{37}$$

$$\|\boldsymbol{q} - \boldsymbol{q}_h\|_0 \leq Ch^{k-1}. \tag{38}$$

Above the constants C do not depend on the plate thickness t which means that the methods are completely free from locking. For the smoothed moment and shear force we naturally have the same error estimates.

4 Numerical examples

4.1 A benchmark problem

The numerical examples will be given for a clamped square plate subject to a uniform load $f = 1$. The side length of the plate equals to unity and the thickness is $t = 0.01$. In the calculations we choose $E = 1$, $\nu = 0.3$ (which gives $G = 5/13$) and $\kappa = 5/6$. Since the thickness of the plate is "small", we will calculate the exact solution to the problem using the classical Kirchhoff plate model.

Due to the symmetry, only one quadrant of the plate is discretized. The computational domain is divided uniformly into $N \times N$ quadrilaterals (or $2N \times N$ triangles). Examples of the finite element meshes (for the case $N = 4$) are shown in Figures 1 and 2.

We will consider Methods I-III with $k = 1, 2$ and rename them according to Table 1 below. Note that both Methods II & III give the same element, namely the STAB4, when $k = 1$.

Table 1. Abbreviations for the different methods.

	Method I	Method II	Method III
$k = 1$	STAB3	STAB4	STAB4
$k = 2$	STAB6	STAB9	STAB8

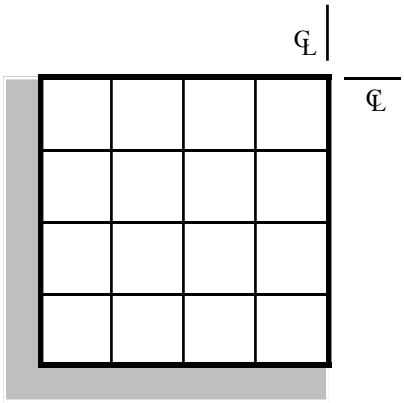

Figure 1. The square plate mesh with $N = 4$ for quadrilateral elements.

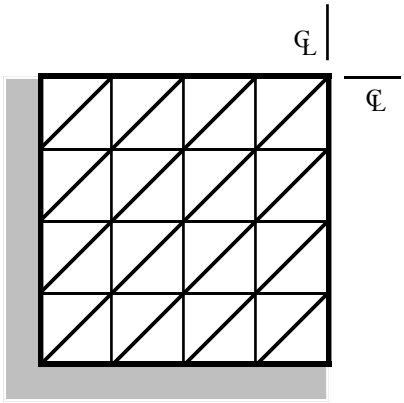

Figure 2. The square plate mesh with $N = 4$ for triangular elements.

In all test cases we choose $\alpha = 0.2$ for the STAB3 element and $\alpha = 0.1$ for the STAB4 element. For the STAB6, STAB8 and STAB9 elements we choose $\alpha = 0.05$. As h_K we take the largest side length of the elements.

In Tables 2-4 below the normalized centerpoint deflections for different elements are shown. Tables 5-7 give the normalized L_2-errors for the deflection.

Table 2. The normalized center point deflection $w_h(\text{center})/w(\text{center})$ for the linear and bilinear elements.

N	STAB3	STAB4	MITC4
4	1.0682	1.0484	0.9885
8	1.0191	1.0125	0.9971
16	1.0064	1.0032	0.9993

Table 3. The normalized center point deflection $w_h(\text{center})/w(\text{center})$ for the quadratic triangular elements.

N	STAB6	MITC7
2	1.0234	0.9613
4	1.0055	0.9967
8	1.0014	0.9998

Table 4. The normalized center point deflection $w_h(\text{center})/w(\text{center})$ for the quadratic quadrilateral elements.

N	STAB8	STAB9	MITC9
2	1.0176	1.0144	0.9996
4	1.0031	1.0006	1.0019
8	1.0007	1.0001	1.0006

Table 5. The errors $||w - w_h||_0/||w||_0$ for the linear and bilinear elements.

N	STAB3	STAB4	MITC4
4	0.0809	0.0360	0.0720
8	0.0225	0.0096	0.0183
16	0.0074	0.0025	0.0046

Table 6. The errors $||w - w_h||_0/||w||_0$ for the quadratic triangular elements.

N	STAB6	MITC7
2	0.0350	0.0550
4	0.0071	0.0059
8	0.0017	0.0006

Table 7. The errors $||w - w_h||_0/||w||_0$ for the quadratic quadrilateral elements.

N	STAB8	STAB9	MITC9
2	0.0286	0.0224	0.0296
4	0.0047	0.0030	0.0048
8	0.0009	0.0004	0.0009

Tables 8-10 below give the normalized L_2-errors for the smoothed bending moment.

Table 8. The errors $||\boldsymbol{M} - \boldsymbol{M}_h^*||_0/||\boldsymbol{M}||_0$ for the linear and bilinear elements.

N	STAB3	STAB4	MITC4
4	0.1713	0.1811	0.1792
8	0.0632	0.0711	0.0700
16	0.0228	0.0265	0.0261

Table 9. The errors $||\boldsymbol{M}-\boldsymbol{M}_h^*||_0/||\boldsymbol{M}||_0$ for the quadratic triangular elements.

N	STAB6	MITC7
2	0.1110	0.2010
4	0.0301	0.0594
8	0.0078	0.0178

Table 10. The errors $||\boldsymbol{M}-\boldsymbol{M}_h^*||_0/||\boldsymbol{M}||_0$ for the quadratic quadrilateral elements.

N	STAB8	STAB9	MITC9
2	0.1171	0.1150	0.1113
4	0.0332	0.0307	0.0308
8	0.0082	0.0081	0.0082

In Tables 11-13 the normalized L_2-errors for the smoothed shear force are shown. The shear force for the quadratic elements with $k = 2$ has been calculated from (17) and for linear elements with $k = 1$ from (16). Eventhough the error estimates for the two different approximateshear forces are the same, it is our experience that one gets better results from (17) when $k \geq 2$.

Table 11. The errors $||\boldsymbol{Q}-\boldsymbol{Q}_h^*||_0/||\boldsymbol{Q}||_0$ for the linear and bilinear elements.

N	STAB3	STAB4	MITC4
4	0.1415	0.2319	0.2315
8	0.0774	0.1567	0.1561
16	0.0561	0.1096	0.1092

Table 12. The errors $||\boldsymbol{Q}-\boldsymbol{Q}_h^*||_0/||\boldsymbol{Q}||_0$ for the quadratic triangular elements.

N	STAB6	MITC7
2	0.3371	0.4495
4	0.1586	0.2371
8	0.0683	0.1076

Table 13. The errors $||\boldsymbol{Q}-\boldsymbol{Q}_h^*||_0/||\boldsymbol{Q}||_0$ for the quadratic quadrilateral elements.

N	STAB8	STAB9	MITC9
2	0.3360	0.3439	0.3217
4	0.1471	0.1471	0.1418
8	0.0586	0.0594	0.0581

4.2 The accuracy with respect to the parameter α

We will finally study how the accuracy of the stabilized methods depends on the choice of the parameter α. We consider the clamped square plate with $t = 0.01$ and use the uniform mesh with $N = 4$ for the quadratic elements and $N = 8$ for the linear elements.

We recall that for $k \geq 2$ our methods are stable only for $0 < \alpha < C_I$.

In Figures 3-5 the normalized L_2-errors for the deflection, bending moment and shear force are shown for the STAB3 element with respect to the parameter α. As we can see, choosing $\alpha \geq 0.05$ is enough to ensure the stability of the method.

In Figures 6-8 the same calculations are shown for the STAB6 element.

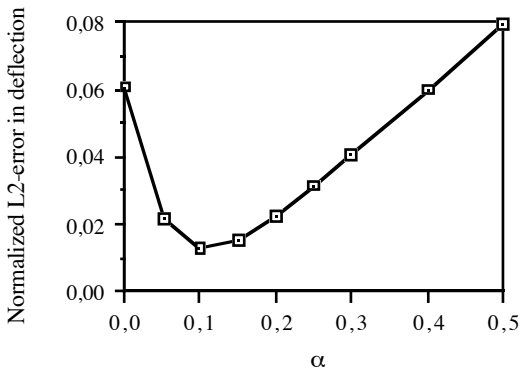

Figure 3. The dependence of the error $||w-w_h||_0/||w||_0$ on the parameter α for the STAB3 element.

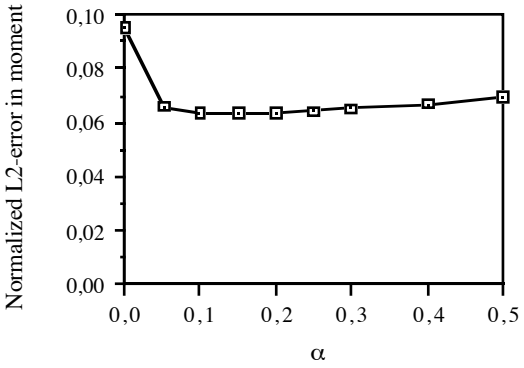

Figure 4. The dependence of the error $||\boldsymbol{M}-\boldsymbol{M}_h^*||_0/||\boldsymbol{M}||_0$ on the parameter α for the STAB3 element.

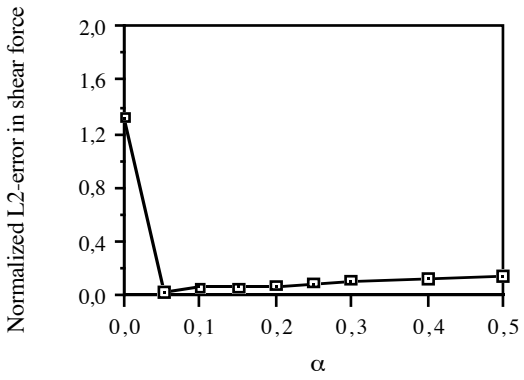

Figure 5. The dependence of the error $||\boldsymbol{Q}-\boldsymbol{Q}_h^*||_0/||\boldsymbol{Q}||_0$ on the parameter α for the STAB3 element.

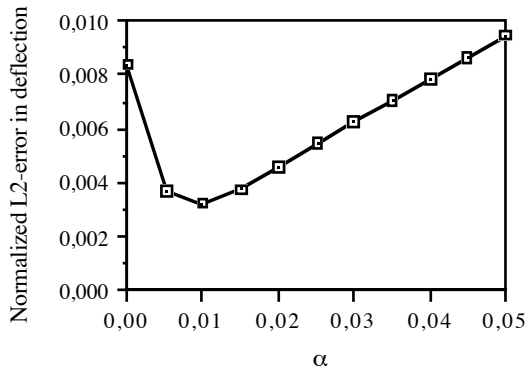

Figure 6. The dependence of the error $||w - w_h||_0/||w||_0$ on the parameter α for the STAB6 element.

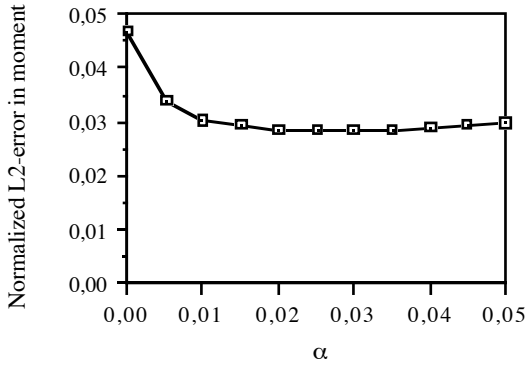

Figure 7. The dependence of the error $||\boldsymbol{M} - \boldsymbol{M}_h^*||_0/||\boldsymbol{M}||_0$ on the parameter α for the STAB6 element.

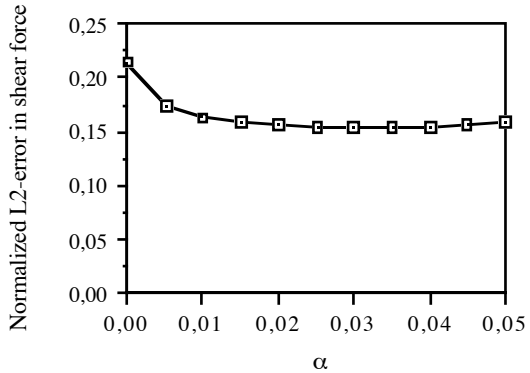

Figure 8. The dependence of the error $||\boldsymbol{Q} - \boldsymbol{Q}_h^*||_0/||\boldsymbol{Q}||_0$ on the parameter α for the STAB6 element.

References

[1] K.J. Bathe, F. Brezzi, and S.W. Cho. The MITC7 and MITC9 plate elements. *Comput. Struct.*, 32:797–814, 1989.

[2] K.J. Bathe, F. Brezzi, and M. Fortin. Mixed-interpolated elements for Reissner-Mindlin plates. *Int. J. Num. Meths. Eng.*, 28:1787–1801, 1989.

[3] K.J. Bathe and E. Dvorkin. A four node plate bending element based on Mindlin-Reissner plate theory and mixed interpolation. *Int. J. Num. Meths. Eng.*, 21:367–383, 1985.

[4] F. Brezzi and M. Fortin. *Mixed and Hybrid Finite Element Methods.* Springer-Verlag, 1991.

[5] F. Brezzi, M. Fortin, and R. Stenberg. Error analysis of mixed-interpolated elements for Reissner-Mindlin plates. *Mathematical Models and Methods in Applied Sciences*, 1:125–151, 1991.

[6] F. Brezzi, J. Douglas Jr., M. Fortin, and L.D. Marini. Efficient rectangular mixed finite elements in two and three space variables. M^2AN, 21:237–250, 1987.

[7] T.J.R. Hughes and R. L. Taylor. The linear triangular plate bending element. In J. R. Whiteman, editor, *The Mathematics of Finite Elements and Applications IV. MAFELAP 1981*, pages 127–142. Academic Press, 1982.

[8] M. Lyly, R. Stenberg, and T. Vihinen. A stable bilinear element for Reissner-Mindlin plates. *Comp. Meths. in Appl. Mech. Engrg.*, 110:343–357, 1993.

[9] E. Oñate, O.C. Zienkiewicz, B. Suarez, and R.L. Taylor. A general methodology for deriving shear constrained Reissner-Minldlin plate elements. *Int. J. Num. Meths. Eng.*, 33:345–367, 1992.

[10] P.A. Raviart and J.M. Thomas. A mixed finite element method for second order elliptic problems. In *Mathematical Aspects of the Finite Element Method. Lecture Notes in Math. 606*, pages 292–315. Springer-Verlag, 1977.

[11] R. Stenberg. A new finite element formulation for the plate bending problem. Helsinki University of Technology, Laboratory for Strength of Materials. Report 17, 1993. To be published. In L. Trabucho, editor, *Proceedings of the International Conference on Asymptotic Methods for Elastic Structures. Lisbon, October 4-8, 1993.*